See page 1006

Preclinical Differences of Intravascular AAV9 Delivery to Neurons and Glia: A Comparative Study of Adult Mice and Nonhuman Primates

Steven J Gray[1], Valerie Matagne[2], Lavanya Bachaboina[1], Swati Yadav[1], Sergio R Ojeda[2] and R Jude Samulski[1]

[1]Gene Therapy Center, University of North Carolina at Chapel Hill, Chapel Hill, North Carolina, USA; [2]Division of Neuroscience, Oregon National Primate Research Center, Beaverton, Oregon, USA

Other labs have previously reported the ability of adeno-associated virus serotype 9 (AAV9) to cross the blood-brain barrier (BBB). In this report, we carefully characterized variables that might affect AAV9's efficiency for central nervous system (CNS) transduction in adult mice, including dose, vehicle composition, mannitol coadministration, and use of single-stranded versus self-complementary AAV. We report that AAV9 is able to transduce approximately twice as many neurons as astrocytes across the entire extent of the adult rodent CNS at doses of 1.25×10^{12}, 1×10^{13}, and 8×10^{13} vg/kg. Vehicle composition or mannitol coadministration had only modest effects on CNS transduction, suggesting AAV9 crosses the BBB by an active transport mechanism. Self-complementary vectors were greater than tenfold more efficient than single-stranded vectors. When this approach was applied to juvenile nonhuman primates (NHPs) at the middle dose ($9–9.5 \times 10^{12}$ vg/kg) tested in mice, a reduction in peripheral organ and brain transduction was observed compared to mice, along with a clear shift toward mostly glial transduction. Moreover, the presence of low levels of pre-existing neutralizing antibodies (NAbs) mostly occluded CNS and peripheral transduction using this delivery approach. Our results indicate that high peripheral tropism, limited neuronal transduction in NHPs, and pre-existing NAbs represent significant barriers to human translation of intravascular AAV9 delivery.

Received 10 December 2010; accepted 20 March 2011; published online 12 April 2011. doi:10.1038/mt.2011.72

INTRODUCTION

A significant barrier to central nervous system (CNS) gene delivery is the blood-brain barrier (BBB), which prevents large or hydrophobic molecules such as viruses, large drugs, and many proteins from passively crossing into the brain. The BBB consists of three layers that separate the brain/spinal cord and cerebrospinal fluid from the blood, and is primarily localized to the unique tight junctions of endothelial cells.[1,2] These layers, called the cerebral capillary endothelium, choroids plexus epithelium, and arachnoid membranes, are each composed of a layer of cells connected by tight junctions. As early as 2003, transient disruption of the BBB with mannitol was reported to allow adeno-associated virus serotype 2 (AAV2) transduction of neural cells after intravenous delivery.[3–5] Interestingly, recent reports have demonstrated some ability of AAV9 and AAV6 to enter the CNS following intravenous (i.v.) delivery without the use of any BBB-permeabilizing agents.[6–9] Particularly with AAV9, there is conflicting data on whether neurons are transduced after intravenous delivery in adults. Moreover, most of the descriptions are focused on spinal cord delivery. Duque *et al.* reports 5–19% of motor neurons transduced in adult mice at a dose of 1×10^{14} viral genomes (vg)/kg,[6] whereas Foust *et al.* reports ~5% at a higher dose of 2×10^{14} vg/kg.[7] Encouragingly, AAV9 was also shown to transduce neural cells after intravenous delivery in adult cats[6] and one newborn cynomolgus macaque.[9] Although not described in either report, a potential limitation of this approach is the high degree of vector delivery to organs outside the CNS such as liver, heart, kidney, and skeletal muscle.[10]

The existing reports on AAV intravascular delivery to the brain have all used self-complementary (sc) AAV vectors, which utilize a mutant AAV2 inverted terminal repeat on one side of the transgene, to package two complementary copies of the transgene linked in *cis* with the mutant inverted terminal repeat and flanked by wild-type AAV2 inverted terminal repeats.[11,12] scAAV vectors are 10–100-fold more efficient than traditional single-stranded (ss) AAV vectors, but they have the capacity to package only about 2.2 kb of foreign DNA, compared to 4.5 kb for ssAAV vectors.

In this study, we sought to investigate in detail the variables that might influence the efficiency of AAV9 delivery to the CNS, for research or translational purposes. These include the potential effects of mannitol or the buffer formulation of the vector vehicle on delivery efficiency. To assess the true packaging constraints with this approach, we compared ssAAV vectors to scAAV vectors. We also sought to examine variables that would influence

The first two authors contributed equally to the work.

Correspondence: *Steven J Gray, Gene Therapy Center, University of North Carolina at Chapel Hill, 7119 Thurston Bowles, CB 7352, Chapel Hill, North Carolina 27599-7352, USA. E-mail: graysj@email.unc.edu*

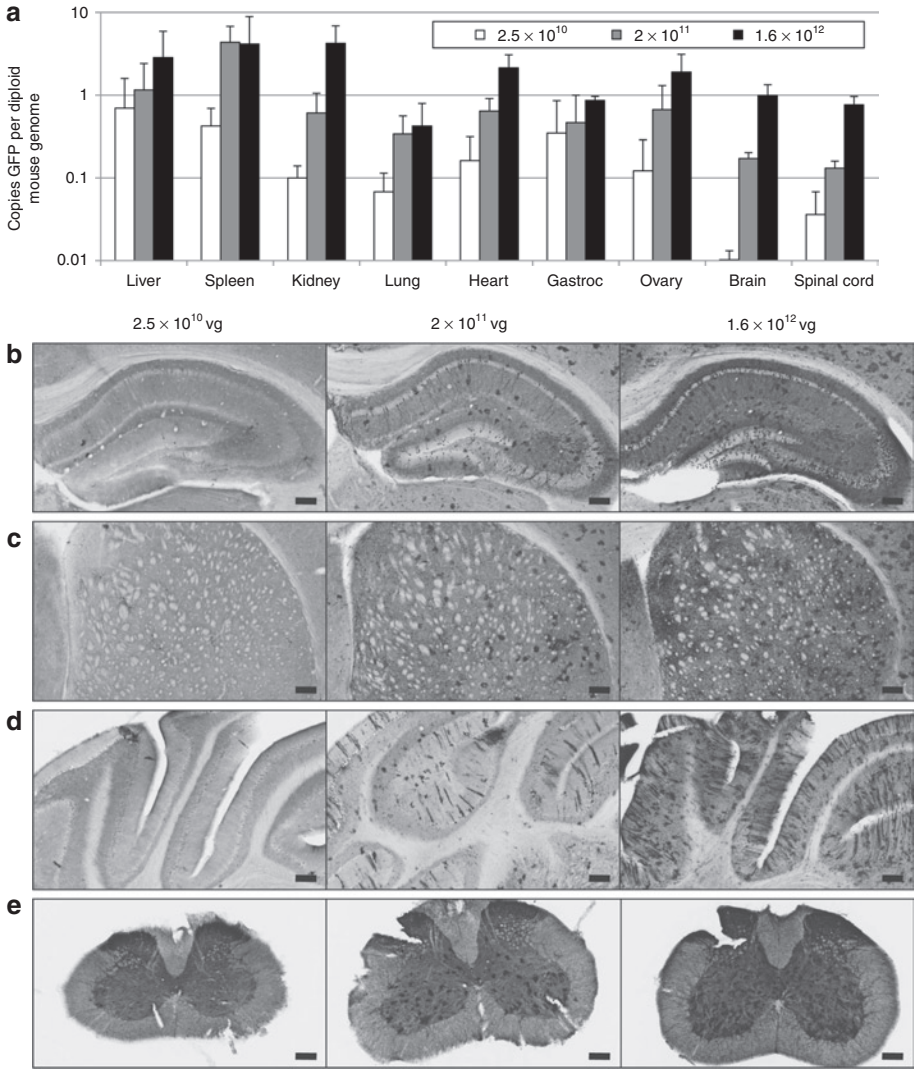

Figure 1 Dose response of mouse central nervous system (CNS) transduction and biodistribution of adeno-associated virus serotype 9 (AAV9). (**a**) Mice were injected with scAAV9/CBh-GFP at the indicated doses, then killed 4 weeks later for quantitative PCR biodistribution and immunohistochemistry to detect green fluorescent protein (GFP) in the (**b**) hippocampus, (**c**) striatum, (**d**) cerebellum, and (**e**) spinal cord. In **b**–**e**, the left panel shows 2.5×10^{10} vg (1.25×10^{12}vg/kg), the middle panel shows 2×10^{11} vg (1×10^{13}vg/kg), and the right panel shows 1.6×10^{12}vg (8×10^{13}vg/kg). All 3,3′-diaminobenzidine tetrachloride (DAB) staining reactions were done in parallel for the same amount of time. In **a**, error bars indicate standard deviation. (**b**–**e**) Bar = 200 µm. Negative control tissue, magnified images, and longer DAB exposures for the high dose are provided as **Supplementary Figures S2–S8**. Fold expression values and corresponding *P* values of organs relative to the brain and spinal cord can be found in **Supplementary Table S1**.

the translational feasibility of an AAV9 intravascular approach, namely the vector biodistribution, dose response, and efficacy in adult mice and juvenile nonhuman primates (NHPs).

RESULTS

AAV9 achieves robust delivery to neurons and glia after i.v. CNS delivery in adult mice

To assess the ability of AAV9 to transduce neural cells after i.v. delivery, adult mice were injected, via the tail vein, with either 2.5×10^{10}, 2×10^{11}, or 1.6×10^{12} vg of scAAV9/CBh-GFP (1.25×10^{12}, 1×10^{13}, and 8×10^{13} vg/kg, respectively). Four weeks later, mice were killed and assessed for brain and spinal cord transduction and vector biodistribution. We also tested AAV1, AAV5, AAV6, and AAV8 for CNS transduction after tail vein injection compared to AAV9. Although AAV6 displayed a small level of CNS transduction and AAV8 was somewhat better, none of these serotypes were as efficient as AAV9 (**Supplementary Figure S1**). After AAV9 delivery, green fluorescent protein (GFP) positive cells were visible in unstained brain and spinal cord sections by viewing native GFP fluorescence (data not shown). However, GFP immunohistochemistry (IHC) coupled with a Vectastain ABC secondary detection kit provided greater sensitivity with minimal background (**Supplementary Figure S2**). Transduction of all brain areas and spinal cord was apparent in a dose-responsive manner with AAV9, with neurons outnumbering astrocytes in the hippocampus (2.0:1) and striatum (1.9:1), but not cortex (1.0:1) (**Figures 1,2 and 3**, **Supplementary Table S2** and **Supplementary Figures S3–S8**). As expected, structures

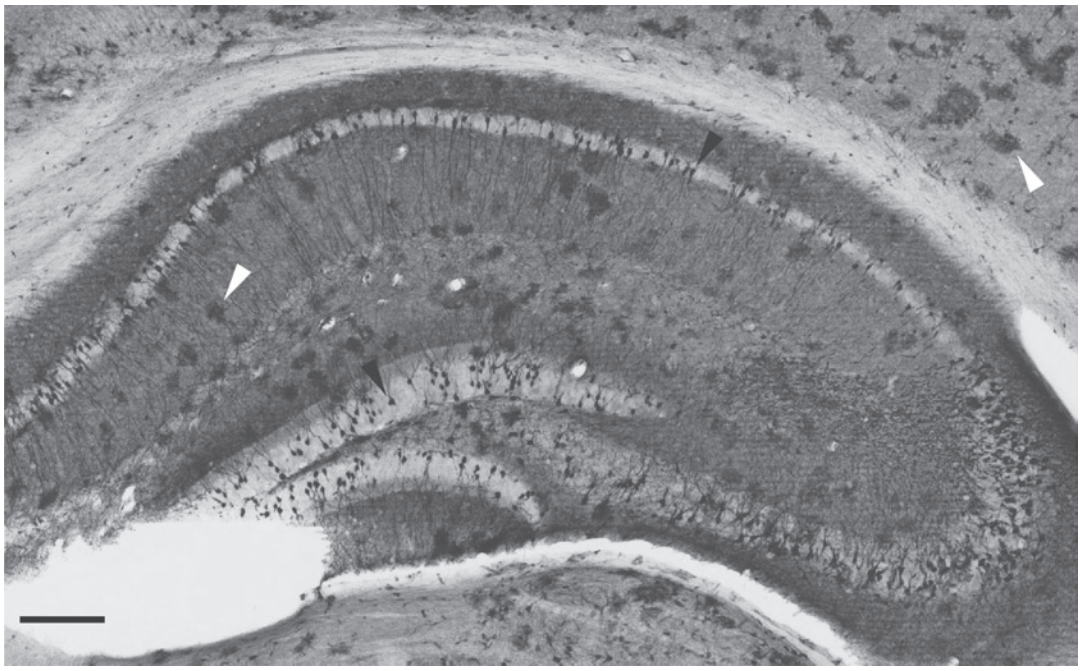

Figure 2 Efficient transduction of neurons and glia in the mouse hippocampus. Enlarged image of **Figure 1b**, right panel. Bar = 200 µm. Arrowheads indicate examples of cells with neuronal (black) or glial (white) morphology.

outside of the BBB (such as the median eminence, **Figure 3f**) show higher overall transduction. Co-immunofluourescent labeling with antibodies against glial fibrillary acidic protein (astrocytes), NeuN (neurons), calbindin (Purkinje neurons), and ChAT (motor neurons) showed that AAV9 efficiently transduced a mix of mostly neurons and astrocytes (**Figure 4**). A small degree of co-labeling was also seen between GFP and Olig1 (oligodendrocytes), but not CD11b (microglia) (data not shown). From the same mice, portions of the brain, spinal cord, liver, heart, kidney, spleen, ovary, and gastrocnemius muscle were used for DNA extraction and quantitation of the GFP transgene by quantitative PCR (qPCR, **Figure 1**). All GFP quantitation was normalized to the quantitation of a genomic reference in the laminB2 locus, to determine the number of GFP copies per diploid mouse genome. The kidney, brain, and spinal cord biodistribution escalated in a linear fashion correlating with dose. Other tissues, in particular the liver, spleen, lung, and skeletal muscle, did not follow a linear escalation of GFP copies correlating to dose, indicating possible saturation of AAV9's transduction capability in these tissues at the middle or high dose.

The vehicle composition, but not mannitol, affects AAV9 CNS transduction and biodistribution

Mannitol can aid large molecules to passively enter the CNS, by transiently loosening the tight junctions between endothelial cells. To test whether mannitol preinjection can help AAV9's penetration of the CNS as it can for AAV2,[4,5] adult mice were injected in the tail vein with 2×10^{11} vg (1×10^{13} vg/kg) of scAAV9/CBA-GFP with or without a prior tail vein injection of a 25% mannitol solution (200 µl). After 4 weeks, the mice were killed and their brains were taken for qPCR biodistribution. As assessed by copies of GFP per diploid mouse genome, coadministration of mannitol 8 minutes prior to AAV injection resulted in only a 50% increase in brain delivery (**Figure 5a**). Time points of 1, 5, and 10 minutes were also tested with little to no effect on AAV9 CNS transduction (data not shown).

To test whether the vehicle solution of AAV9 might affect the CNS transduction and/or biodistribution, a stock solution of scAAV9/CMV-GFP in a buffer of 1 × phosphate-buffered saline (PBS), 5% sorbitol, and 213 mmol/l added NaCl (350 mmol/l final NaCl concentration) was diluted to the final buffer compositions shown in **Figure 5b**. Then 1×10^{11} vg (5×10^{12} vg/kg) was injected via the tail vein into adult mice. After 4 weeks, the mice were killed and the brains and spinal cords were recovered for qPCR biodistribution. The presence of 5% sorbitol in the vehicle increased transduction in the CNS approximately twofold. Increasing the vehicle NaCl concentration up to 350 mmol/l further enhanced AAV delivery to the brain and spinal cord, but this effect was lost as the NaCl concentration was increased to 480 mmol/l. These results demonstrate that modifying the AAV9 vehicle composition can result in greater than a threefold change in brain delivery after tail vein injection in adult mice.

scAAV9 is much more efficient than ssAAV9 for intravascular CNS delivery

The 2.2 kb packaging constraints of scAAV vectors set strict size limits on the genes that could be delivered to the brain by an intravascular approach for research or therapeutic purposes. To test the ability of ssAAV vectors to deliver a larger transgene to the brain by this approach, 5×10^{11} vg (2.5×10^{13} vg/kg) of ssAAV9/CMV-GFP was injected into the tail vein of adult mice. After 4 weeks, the mice were killed and their brains and spinal cords were sectioned for IHC against GFP. Although some transduction of cells with neuronal and glial morphology was visible

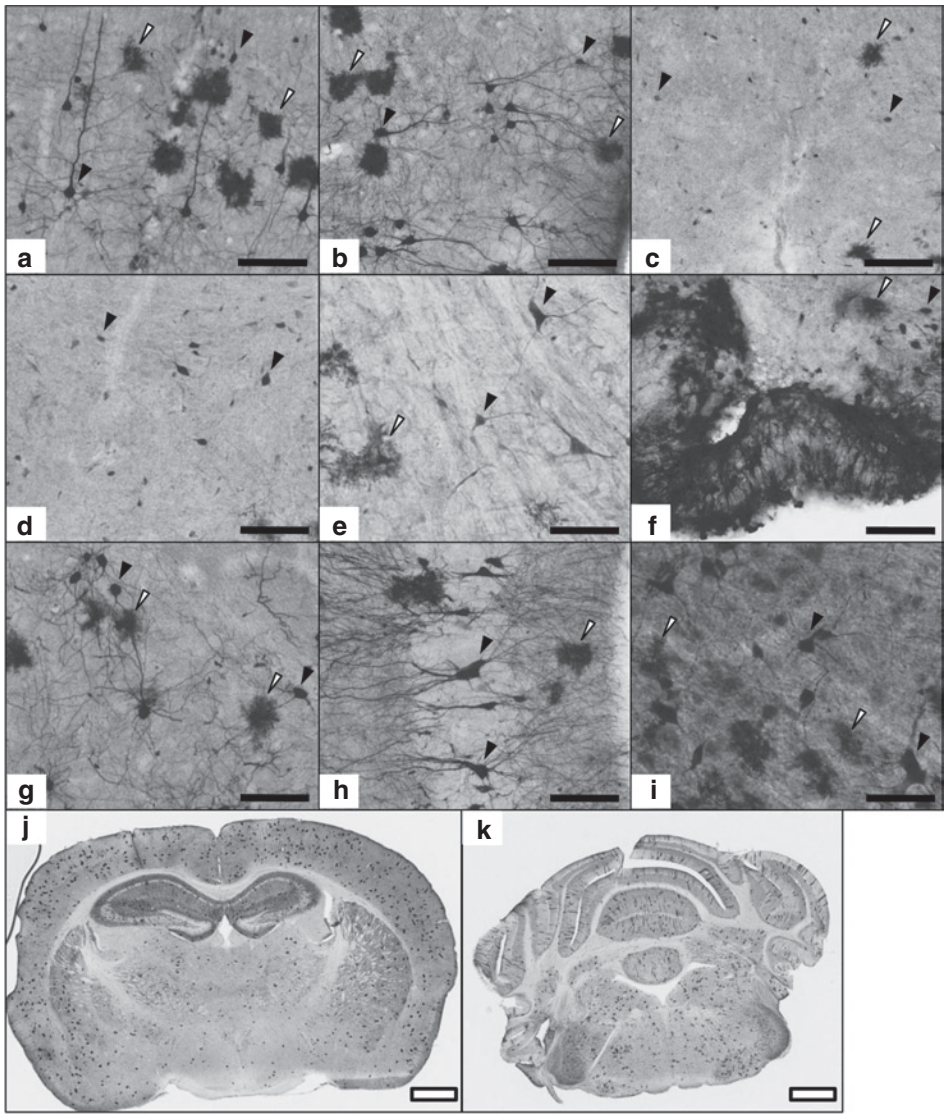

Figure 3 Broad distribution of neuronal and glial transduction across the mouse central nervous system (CNS). Representative images showing immunohistochemistry using an anti-green fluorescent protein (GFP) antibody on coronal brain and spinal cord sections. These were taken from the same set of mice depicted in **Figure 1**, at the 2×10^{11} vg dose (scAAV9/CBh-GFP injected i.v. in adult mice). (**a**–**i**) Filled scale bars are 100 µm, and (**j**,**k**) open scale bars are 1 mm. Filled black arrowheads indicate examples of cells with neuronal morphology, and open (white) arrowheads indicate examples of cells with astrocytic morphology. (**a**) Primary motor cortex, (**b**) piriform cortex, (**c**) hypothalamus, (**d**) thalamus, (**e**) medulla, (**f**) arcuate nucleus and median eminence, (**g**) amygdala, (**h**) caudal hippocampus, (**i**) ventral horn of the cervical spinal cord, (**j**) coronal section, bregma –1.9 mm, (**k**) coronal section, bregma –6.2 mm.

in the brain and spinal cord, it was highly reduced compared to scAAV9 vectors (**Supplementary Figure S9**). The number of GFP-positive cells were similar to those seen with a 20-fold lower dose of 2.5×10^{10} vg of scAAV9 (**Figure 1**), demonstrating the greater efficacy of scAAV9 over ssAAV9.

GFP, but not AAV9, causes transient liver toxicity in mice after i.v. AAV9 administration

To assess the potential consequences of AAV9 intravascular administration and gene expression in naive mice, we injected adult mice with either 2.4×10^{11} vg of ssAAV9/CBA-GFP or 3×10^{11} vg of ssAAV9/CBA-GAN. The giant axonal neuropathy (GAN) construct packages the coding sequence for the protein gigaxonin, which is missing in patients with GAN.[13,14] At 1, 2, 4, 8, 12, and 16 weeks after virus administration, blood was collected and used to measure serum levels of albumin (general inflammation), blood urea nitrogen (kidney toxicity), and alanine amino transferase (ALT, liver toxicity). Weight measurements were also taken at regular intervals up to 60 weeks postinjection, and a group was killed at 4 weeks postinjection to assess vector biodistribution. These results are summarized in **Figure 6**. Neither GFP nor GAN AAV9 vectors caused any significant change in albumin or blood urea nitrogen levels. However, the GFP vector (but not GAN) caused a transient rise in ALT levels that correlated to a significant decrease in GFP genomes detected in the liver. There was no difference in weight between the groups, suggesting that the transient liver toxicity had only minor effects on overall health.

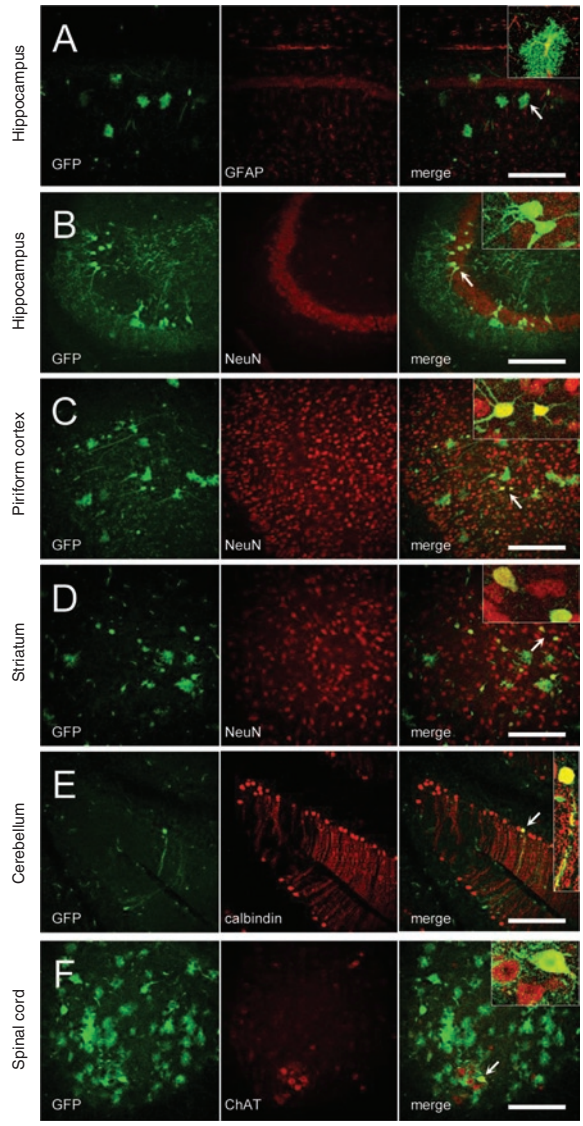

Figure 4 Adeno-associated virus serotype 9 (AAV9) transduces a variety of cell types after i.v. delivery to the mouse central nervous system (CNS). (**a**–**f**) Alternate serial sections described in **Figure 1** were subjected to co-immunofluorescence with the indicated antibodies. For each set of three panels, the left panel shows green fluorescent protein (GFP) expression, the middle shows labeling with the indicated antibody, and the right panel shows a merged image. The inset in the right panel highlights co-localization observed, and the arrow points to the cells magnified. All images are four merged confocal Z-stacks of samples from mice injected with 2×10^{11} vg (1×10^{13} vg/kg), except for panel **f** which shows the 1.6×10^{12} vg (8×10^{13} vg/kg) dose. Note that with panel **e**, native fluorescence was used to visualize GFP expression. Scale bars for all panels are shown in the right panels. Bar = 200 µm.

The success of AAV9 intravascular delivery in juvenile NHPs is dependent on the absence of pre-existing NAbs

To determine whether systemic delivery of AAV9 to NHPs would result in transduction of CNS cells as it does in mice, we conducted a comparison of scAAV9/CBh-GFP transduction efficiency when delivered either by i.v. (saphenous vein, 9×10^{12} vg/kg) or intra-arterial injection (i.c., carotid artery, 9–9.5 $\times 10^{12}$ vg/kg) in 3–4-year-old male rhesus macaques. Two animals were injected by each route, and one i.c. animal (#26706) had a low (1:4) titer of pre-existing AAV9 NAbs. All animals tolerated the procedure well and were in good health until the end of the study. Four weeks after virus infusion, the animals were euthanized and their brains, spinal cords, and several peripheral organs were rapidly dissected and processed for molecular analysis, IHC, and co-IF analysis. GFP immunostaining showed one i.v. NHP (#26945) and one i.c. NHP (#26149) had efficient brain transduction, whereas the other two showed minimal brain transduction (i.c. #26706, i.v. #26165, **Figure 7**). Based on morphology and co-IF, it appears that most GFP-expressing (GFP^+) cells in the brain are astrocytes, which outnumber neurons in the hippocampus (4:1), frontal and parietal cortices (an average of 30:1 and 11:1, respectively), but not in the cerebellum (1:1) (**Figures 7** and **8**, **Supplementary Table S2**, and **Supplementary Figures S10–S12**).

Since NHP 26706 had a pre-existing NAb titer of 1:4, we hypothesized that the poor CNS transduction might be related to an anti-AAV immune response, as has been reported for liver transduction.[15,16] To test this, sera collected at preinjection and 1, 2, and 4 weeks postinjection were examined for AAV9 NAbs. The NHPs 26149 and 26945, with high transduction, had peak NAbs of 1:32 and 1:64, whereas the i.c. NHP (26706) with minimal transduction had a peak NAb titer of 1:512 (**Table 1**). Interestingly, the NAb titer of the i.v. NHP with lower transduction (26165) was low on week 1 (1:64) and kept rising through week 4 (1:256). Correlating with the presence of pre-existing AAV9 NAbs and the hypothesis of NAb-mediated clearance of AAV9 particles, there was a 100-fold decrease in circulating AAV vector genomes at 6 hours postinjection in NHP 26706 with a 1:4 titer of pre-existing NAbs, and no vector genomes were detected at 24 hours postinjection, compared with 1.3×10^6 to 2.6×10^6 vg for the three animals without pre-existing NAbs (**Supplementary Table S3**). The low transduction of NHP 26165, which had no detectable pre-existing NAb but a gradually increasing NAb titer postinjection, had serum titers of AAV particles equivalent to the highly transduced NHPs (26945 and 26149), which suggest a different mechanism to limit transduction than rapid clearance from the blood.

In peripheral tissues, the liver, heart, and adrenals were highly transduced, whereas the kidney, spleen, and testes expressed lower levels of GFP (**Figure 9**). Except for NHP 26706 with pre-existing NAbs, qPCR analysis of AAV9 vector genome biodistribution generally correlated with the GFP expression seen by IHC (**Figure 9**). The i.c.-injected animal with detectable pre-existing NAbs (26706) had little GFP in any peripheral organs, with qPCR showing the highest concentration of vector genomes in the spleen. Interestingly, by peripheral GFP expression and vector biodistribution NHP 26165 showed no apparent deficits, even though CNS transduction was highly reduced and there was a high concentration of vector genomes in the spleen.

DISCUSSION

Intravascular AAV9 delivery to the CNS could possibly have enormous clinical relevance for a number of diseases, such as lysosomal storage diseases and spinal muscular atrophy. The use of the vasculature allows even and widespread CNS gene delivery with a minimally invasive procedure. However, previous studies do not adequately address the translational feasibility of using intravascular AAV9

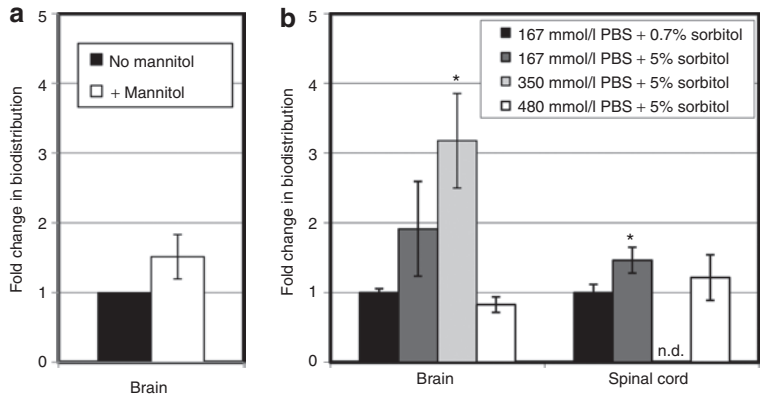

Figure 5 Mannitol and vehicle can modestly affect adeno-associated virus serotype 9 (AAV9) mouse central nervous system (CNS) delivery. In each case, mice received a tail vein injection of 1×10^{11} vg (5×10^{12} vg/kg) of scAAV9/GFP. After 4 weeks, tissues were harvested, and extracted DNA tested by quantitative PCR as described in the methods. (**a**) Mice received an intravenous (i.v.) injection of mannitol 8 minutes prior to i.v. vector injection. (**b**) A virus stock was diluted to create the vehicle compositions shown, then intravenously injected into mice. Error bars indicate standard deviation. n.d., no data. *$P < 0.05$ compared to 167 mmol/l phosphate-buffered saline + 0.7% sorbitol (Student's *T*-test: two-tailed, unpaired, equal variance).

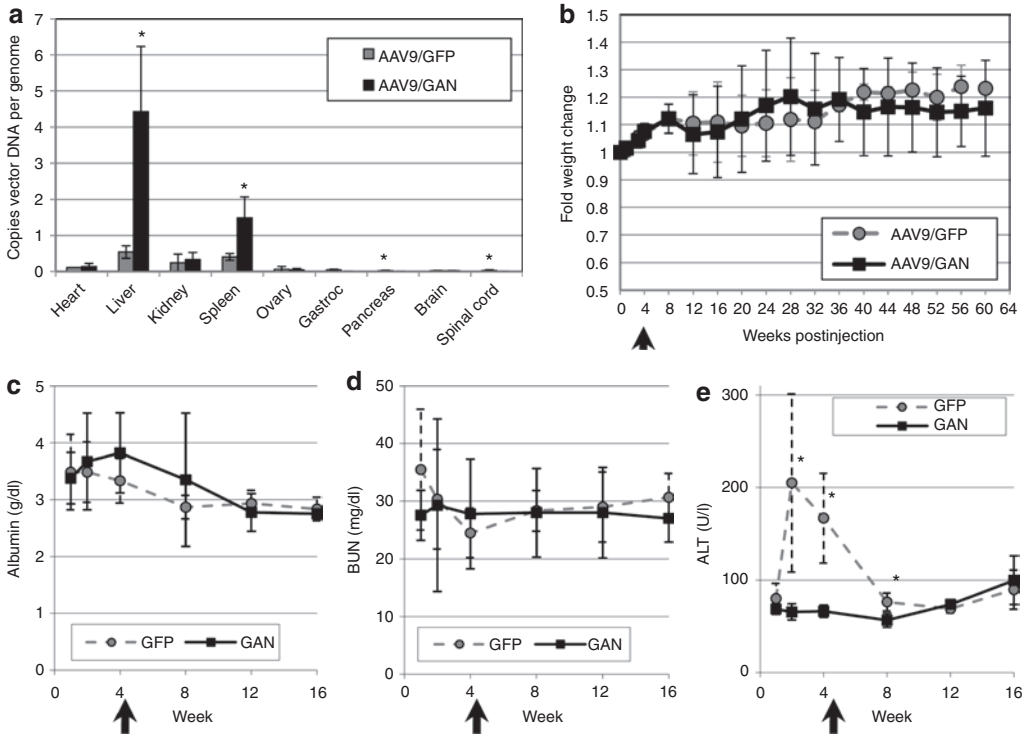

Figure 6 AAV9/GFP, but not AAV9/GAN, vectors show a transient liver toxicity and reduction in vector genomes. Mice were injected with either ssAAV9/CBA-GFP ($n = 6$) or ssAAV9/CBA-GAN ($n = 8$). (**a**) Just after the 4-week time point postinjection, a group of mice ($n = 3$ green fluorescent protein (GFP), $n = 4$ giant axonal neuropathy (GAN)) was killed to assess biodistribution by quantitative PCR. In panels **b**–**e**, the arrow denotes the time when these mice were removed from the cohorts. (**b**) Weights were taken at the indicated time points and expressed relative to the starting weight. Serum was collected at the indicated time points and tested for levels of (**c**) albumin, (**d**) blood urea nitrogen (BUN), and (**e**) alanine amino transferase (ALT). All error bars indicate standard deviation. *Significantly higher value with $P < 0.05$ (Student's *t*-test: two-tailed, unpaired, equal variance). AAV9, adeno-associated virus serotype 9.

delivery to the CNS. To bridge this gap, we report the ability of AAV9 to transduce neurons and glia in the brain and spinal cord of mice and NHPs, along with a quantitation of the dose-responsive delivery to peripheral organs. We also report the efficacy of AAV9 CNS transduction in juvenile NHPs, and the importance of pre-existing NAbs (or more correctly, lack thereof) for efficient intravascular CNS delivery.

An important consideration for any systemic CNS delivery strategy is the amount of vector that enters non-CNS organs. In a recent clinical trial for hemophilia B, the capsid of a rAAV2/factor IX vector delivered to the liver elicited an asymptomatic immune clearance of the vector at doses of 4×10^{11} vg/kg or 2×10^{12} vg/kg.[17–19] In a separate clinical trial for hemophilia B, this

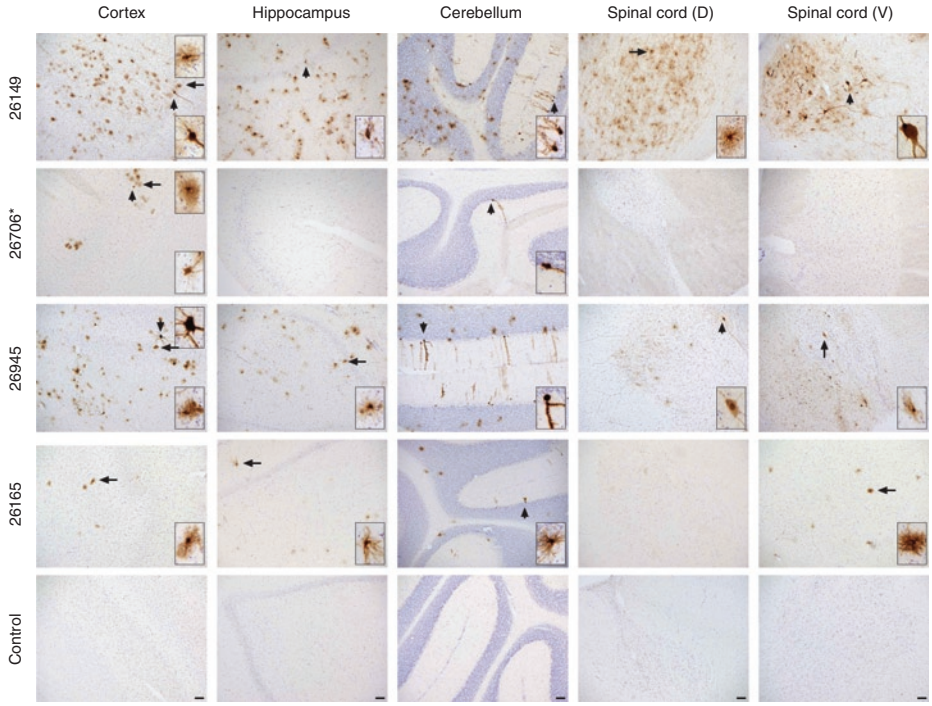

Figure 7 Intravascular injection of adeno-associated virus serotype 9 (AAV9) in nonhuman primates (NHPs) results in broad central nervous system central nervous system (CNS) transduction that is limited by an anti-AAV9 immune response. NHPs were injected with scAAV9/CBh-GFP via the carotid artery (i.c., animals 26149 and 26706) or the saphenous vein (intravenous, animals 26945 and 26165). Green fluorescent protein (GFP) biodistribution was assessed by immunohistochemistry 4 weeks after injection. Examples of GFP expression detected by 3,3′-diaminobenzidine tetrachloride staining in the cortex, hippocampus, cerebellum, dorsal (D) and ventral (V) spinal cord are shown for each animal. Arrows point to GFP-positive cells highlighted in the magnified insets with neuronal (short arrow) or glial (long arrow) morphology. An asterisk (*) denotes that NHP 26706 had detectable pre-existing neutralizing antibodies (see **Table 1**). Bar = 100 µm.

immune response was not observed in the muscle at doses up to 1.8×10^{12} vg/kg, where the rAAV2 vector was well tolerated and transgene expression persisted for over 3 years.[18,20,21] The experience gained from these hemophilia clinical trials suggests liver, but not muscle, transduction as a major barrier to systemic delivery in humans, a finding that was not originally predicted by animal models. In our mouse studies, AAV9 showed the highest tropism for liver, followed by the kidney and spleen. Regardless of dose, the transduction efficiency of AAV9 for CNS delivery was considerably lower than for peripheral organs. Interestingly, although the biodistribution in the brain and spinal cord increased as a function of dose, biodistribution in the liver only increased in approximately twofold increments whereas the dose increased in eightfold increments. This could suggest that although AAV9 receptors did not become saturating in the brain and other tissues, AAV9 receptors in the liver were saturated at higher doses. Although our data do not exclude this possibility, the observed transient rise of ALT in serum (**Figure 6e**) suggests, instead, that many AAV9 particles have entered the liver and been cleared, and the AAV9 biodistribution we observed at 4 weeks is an underestimate of the total AAV genomes that were delivered. In agreement with this hypothesis, when we previously reported GFP biodistribution in mice with AAV9 at 10 days postinjection at 5×10^{10} vg/mouse,[22] there were 30.6 copies of GFP per diploid mouse genome. In this study, looking at 4 weeks postinjection, only 1.2 and 2.8 copies of GFP/genome were detected at vector doses of 2×10^{11} and 1.6×10^{12} vg/mouse, respectively (**Figure 1**). A transient rise in ALT levels was observed when the transgene was GFP but not gigaxonin, and this correlated with less copies of GFP in the liver after 4 weeks (**Figure 6a**), suggesting that GFP was the toxic agent rather than AAV9. Since GFP is a foreign protein and mice would be pre-exposed to their own gigaxonin epitopes (98% identical to human), it is reasonable to propose that AAV9 liver transduction might lead to a cytotoxic T lymphocytes-mediated clearance of GFP-expressing cells. This effect might be a consequence of the mouse strain used, since BALB/c mice are particularly sensitive to a transgene-specific and cytotoxic T lymphocyte-mediated clearance of hepatocytes.[23] The loss of GFP expression might also be a consequence of the serotype used, as Lu and Song demonstrated that AAV1 elicited strong cellular and humoral immune responses to its transgene whereas AAV8 did not, and this difference was attributed to AAV1's tropism for dendritic cells.[24] It is unknown whether AAV9 transduces dendritic cells *in vivo*. Although we cannot comment directly on whether GFP toxicity was a result of GFP protein accumulation or an anti-GFP immune response, the observation of transient transgene-related liver toxicity certainly raises a concern over using AAV9 intravascular delivery to transduce the CNS. The implications of high vector delivery to peripheral organs relative to the CNS need to be addressed in any translational approach. Promising developments in vector design[22,25,26] suggest that new vectors could be engineered to limit peripheral tropism and circumvent this concern, particularly with liver-detargeting mutations identified in AAV9.[27]

This study provided a unique opportunity to assess AAV9 performance in adult mice compared to young adult NHPs. The

dose used in our NHP studies was 0.9–0.95 × 10^{13} vg/kg, which is similar to the 1 × 10^{13} vg per kg dose injected into the 20 g mice in our study. In our studies, we observed extensive transduction of neurons and glia throughout the brain and spinal cord in mice, with neurons outnumbering astrocytes ~2:1 in the hippocampus and striatum, and 1:1 in the cortex (**Figures 1–3**, and **Supplementary Table S2**). These results were different from what we found in NHPs, where the overall transduction efficiency was considerably lower and there was mostly glial transduction (see **Supplementary Table S2**). Our qPCR data showed that at comparable doses (~1 × 10^{13} vg/kg), mice had 0.17 (+/− 0.03 SD) copies GFP per cell in the brain (**Figure 1**). The NHPs without

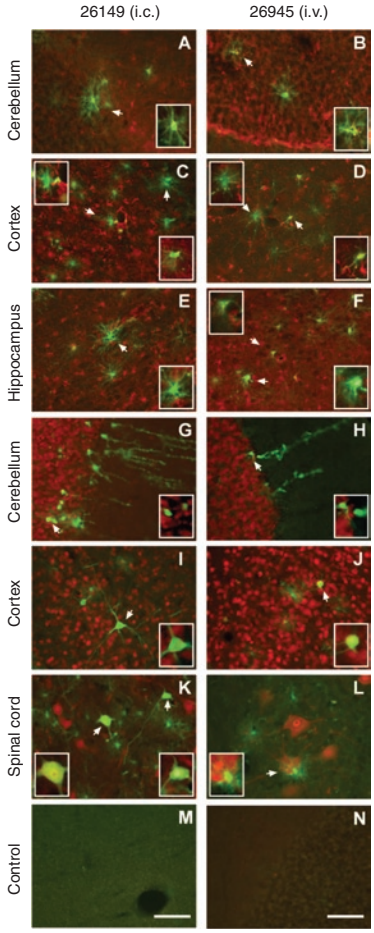

Figure 8 Intravascular adeno-associated virus serotype 9 (AAV9) delivery in nonhuman primates (NHPs) transduces mostly glia in the central nervous system (CNS). Representative sections from the NHPs showing higher levels of transduction (left panels: i.c., 26149; right panels: i.v., 26945) were selected and subjected to co-immunofluorescence with the indicated antibodies. For each picture, green fluorescent protein-expressing cells are green and (**a**–**f**) glial fibrillary acidic protein or (**g**–**l**) NeuN-positive cells are red. Control sections in which no primary antibodies were used are depicted in (**m**) green and (**n**) merged green and red. The insets highlight observed co-localization, arrows pointing to the magnified cells. Scale bars for all panels are on the bottom panels. Bar = 100 µm.

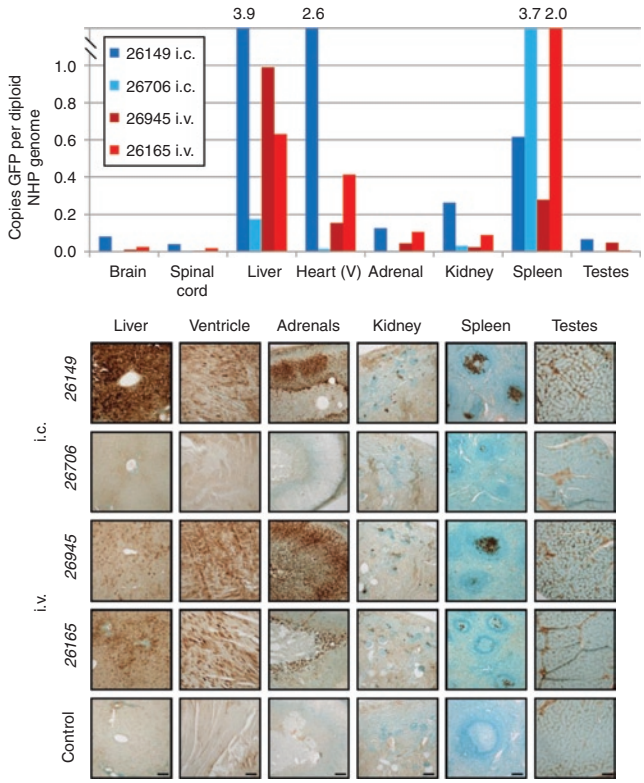

Figure 9 Nonhuman primate (NHP) biodistribution and expression in peripheral organs. At the time of euthanasia, various peripheral organs were rapidly dissected and frozen in liquid nitrogen for quantitative PCR (qPCR) analysis of vector genome biodistribution (top panel) or post-fixed in 4% paraformaldehyde and processed for immunohistochemical detection of green fluorescent protein (GFP) by 3,3′-diaminobenzidine tetrachloride staining (bottom panel). For the qPCR biodistribution studies, the "brain" is the average value of three samples and the "spinal cord" is the average of cervical and lumbar samples. Bottom: animals with no pre-existing antibodies (i.c., 26149; i.v., 26945) showed high levels of transduction in the liver, heart, and adrenals whereas the kidney, spleen, and testes showed lower levels of GFP expression. The animal with pre-existing neutralizing antibodies (NAbs) (i.c., 26706) had no observable GFP expression except in the spleen. The fourth NHP showed rising levels of NAbs throughout the 4 weeks postadministration and had high expression of GFP in the liver, moderate in the heart and adrenals, and low in the kidney, spleen and testes. Scale bar for each organ is shown in the picture of the control sample. Bar = 100 µm.

Table 1 Anti-AAV9 neutralizing antibody titers of the nonhuman primates used in the study

			Neutralizing Ab titer			
Animal ID	**Age (years)**	**Viral titer (vg/kg BW)**	**Preinjection**	**1 week**	**2 weeks**	**4 weeks**
26149 (i.c.)	4	9.5 × 10^{12}	<1:2	1:64	1:64	1:64
26706 (i.c.)	3	8.9 × 10^{12}	1:4	1:512	1:256	1:256
26945 (i.v.)	3	8.7 × 10^{12}	<1:2	1:32	1:32	1:32
26165 (i.v.)	4	9.1 × 10^{12}	<1:2	1:64	1:128	1:256

Abbreviations: Ab, antibody; BW, body weight; i.c., intracarotid; i.v., intravenous.

pre-existing NAbs had significantly less copies per cell in the brain (0.039 +/− 0.037 SD, $P = 0.009$; **Figure 9**), indicating that there is less vector entering or persisting in the brain in NHPs versus mice. At this time, it is unclear what caused the reduction in CNS delivery and neuronal tropism in NHPs as compared to mice. This could be due to any number of species-specific factors including differential BBB transport, capsid-interacting blood factors to promote or inhibit AAV9 transduction (S. Fedor and L. Garcia, Genethon, personal communication, January 2011), neural cell tropism within the brain, and/or intracellular trafficking and vector persistence. In our NHP study, the best CNS and peripheral transduction was observed after i.c. delivery in the absence of pre-existing NAbs. The variability between the two NHPs showing the highest transduction (i.c. 26149 and i.v. 26945) was more than we would normally see with inbred BALB/c mice, but given the difficulty of using large numbers of NHP subjects we cannot yet comment with confidence on whether the i.c. route of administration is indeed better or whether this difference is due to variability between animals. However, these large animal experiments do provide a distinct data collection supporting a unique NHP-specific AAV9 tropism influenced by the route of administration, highlighting the need for additional supporting studies before testing in patients.

In our laboratory and others, when AAV9 is injected intraparenchymally in mice it displays a nearly exclusive neuronal tropism.[7,22,28] The shift in AAV9 toward astrocytic tropism therefore appears to be a result of the route of administration. We can speculate that the passage of AAV9 across the BBB would expose it to endothelial cells, pericytes, and astrocytic processes before it has access to neurons.[1] We could further speculate that whether AAV9 had any ability to transduce these non-neuronal cells, it could explain the shift in tropism when changing the delivery route from intraparenchymal to intravascular delivery. Alternatively, there might be factors in the blood that bind the AAV9 capsid and modify its tropism, as has been previously demonstrated with liver-specific uptake of adenovirus vectors.[29,30] In either case, the ineffectiveness of mannitol to enhance AAV9 CNS transduction in the mouse suggests that AAV9 employs an active transport mechanism across the BBB rather than passively slipping through the tight junctions between endothelial cells.

The efficient transduction of mouse neurons in our studies is in accordance with what was reported by Duque *et al.*, but inconsistent with the report by Foust *et al.*[6,7] We have no explanation for why we saw transduction of neurons in the adult mouse brain and Foust *et al.* did not, but in our experiments, we tested three different promoters with similar results, one of which (CBA) is the same promoter used by Foust *et al.*[7] In addition to the highly pure CsCl gradient-purified vector used for all the reported data, in the course of our studies we also tested vectors purified by ion-exchange chromatography, as well as "dirty" vector preparations containing high amounts of cellular protein contamination (data not shown). We also tested different vehicle compositions and multiple doses (**Figures 1** and **5**). In all cases, we always observed transduction of similar ratios of neurons and glia, with the overall efficiency primarily dependent on dose. It is our conclusion that AAV9 transduces both neurons and glia after intravascular delivery in adult mice and mostly glia in NHPs.

When discussing the translational feasibility of AAV9 intravascular delivery to large animals and humans, vector dose represents a significant translational barrier. Manufacturing vector for rodent studies (both for basic science and preclinical testing) at even a very high dose (2×10^{14} vg/kg) is certainly feasible, and this could be valuable in certain research applications to avoid the time-consuming generation of transgenic mice. When a dose of 2×10^{14} vg/kg is needed in a 5 kg NHP, manufacturing 1×10^{15} vg per animal becomes a significant logistical challenge, especially in a multi-animal study with sufficient numbers for statistical significance. Vector needs for application to multiple 20 kg children or 80 kg adults becomes prohibitive with current manufacturing capabilities. However, the dose of 1×10^{13} vg/kg used in our NHP studies may be more reasonable for translation from a manufacturing standpoint. As the level of CNS transduction seen at these doses is lower than expected when comparing mice to NHPs, further studies are warranted to determine whether an AAV9 intravascular approach may be a realistic therapeutic strategy.

Another translational obstacle is the potential for pre-existing NAbs to the AAV9 capsid, which is estimated to be present in 33.5% of the human population.[31] Although the number of NHPs in our study was too low to draw firm conclusions, two of the NHPs showed minimal CNS transduction, and this correlated with the highest NAb titers following injection. The NHP 26706 with the highest peak NAb titer (1:512) also had a low but detectable titer of pre-existing NAbs (1:4). The pre-existing NAb titer correlated with a more rapid clearance of AAV from the blood, as might be expected from previous findings that low NAbs titers can block liver transduction in NHPs (1:5)[15] and mice (1:10).[32] The uncertainty comes from the second NHP with poor CNS transduction, #26165. This NHP had no detectable pre-existing NAbs and normal serum titers of circulating AAV9 at 6 and 24 hours postinjection (relative to the two successfully transduced NHPs 26149 and 26945), indicating that there was not an initial NAb-mediated clearance of vector. Peripheral organ delivery and transduction were observed, but CNS transduction was minimal and there was a gradual rise in AAV9 NAbs following the injection. From these results, we might speculate that NHP 26165 mounted a delayed immune reaction responsible for the clearance of transduced cells, or else there was another unknown block to CNS transduction in this particular NHP. From our data, we cannot conclude whether there was an initial block to CNS/neural cell infection in NHP 26165, or whether GFP+ cells were specifically cleared only from CNS after successful gene delivery. All together, our results suggest that even a very low pre-existing AAV9 NAb titer presents a clear obstacle to AAV9-mediated CNS delivery in NHPs, and that other uncharacterized barriers might exist that could limit transduction in NHPs. These known and unknown obstacles indicate that further investigation of AAV9 NHP tropism and/or additional engineered capsids[22,26,33,34] are warranted before translation of this approach to humans is pursued.

In conclusion, we report widespread transduction of neurons and glia in the spinal cord and brain of mice after intravenous administration of AAV9 and a predominant transduction of glia in NHPs after both intravenous and intra-arterial administration. The optimization of AAV vectors for intravascular CNS

delivery could have important immediate implications for disorders such as lysosomal storage diseases that would employ intra-CNS expression of secreted enzymes to break down toxic metabolic intermediates, and would not necessarily require high neuronal transduction (see reviews).[35,36] However, the inability of systemically administered AAV9 to efficiently transduce neurons in NHPs diminishes the feasibility of this approach for the treatment of human brain diseases, especially those that would require efficient neuronal transduction such as spinal muscular atrophy, fragile X syndrome, or Rett syndrome. In instances where global transduction is desired but there is a need to restrict expression to only specific sub-populations of neurons (such as Parkinson's Disease), there would be a clear need to either use a cell-specific promoter or to modify the AAV capsid to specifically target those cells. Even if AAV9 is not an ideal vector, there is still the potential for identifying new AAVs, naturally occurring or engineered, which would be more appropriate. For example, liver-detargeting mutations in AAV9 have been identified that may make it more amenable for safe intravascular gene transfer to the CNS.[27] While the ability of AAV9 to transduce the CNS in juvenile NHPs provides additional translational relevance to this approach, the consequences of vector delivery to non-CNS organs, low neuronal transduction efficiency, and potential interference by pre-existing NAbs needs to be addressed.

MATERIALS AND METHODS

Virus preparation. rAAV vectors were produced by the University of North Carolina Vector Core using a triple-transfection method in HEK293 cells as described.[37] Highly pure recombinant virus were recovered using two sequential CsCl gradients, then the peak fractions were dialyzed in PBS containing 5% D-sorbitol, unless otherwise indicated. When scAAV vectors were made, the majority of packaged genomes were full-length self-complementary (data not shown). Viral titers were determined by both dot blot[37] and qPCR. The recombinant vectors in these studies utilized several packaged transgene cassettes: sc-CBA-GFP, sc-CBh-GFP, sc-CMV-GFP, ss-CBA-GFP, and ssCBA-GAN. Details of these constructs can be found in **Supplementary Table S4.**

Quantitative PCR and biodistribution. qPCR was used to determine viral titer and for biodistribution studies. Viral and tissue DNA was purified and quantitated using SyBR Green as described,[22] except for the NHP GAPDH qPCR reactions. Note that for the mouse brain, every 5th coronal section was pooled and used for DNA extraction. Copies of GFP were assessed in each organ sample and normalized to copies of the mouse laminB2 locus or copies of the rhesus GAPDH locus, as appropriate (with two copies of the genomic reference representing a diploid host genome). NHP GAPDH qPCR reactions were done on a Roche 480 Lightcycler instrument using the Faststart Taqman Probe Master Mix (catalog # 4673450001; Roche, Indianapolis, IN), following the manufacturer's instructions. The primer and probe sequences for GAPDH were as follows: forward: 5′-ggcctccaaggagtaagacc-3′, reverse: 5′-tctcttcctcttgtgctctcg-3′, probe: accaccag (catalog # 04694155001, probe #131 UPL extension library).

Mouse studies

All investigations were approved by the University of North Carolina–Chapel Hill Institutional Animal Care and Use Committee. Two hundred microliters of vector of the indicated titers of each serotype were injected into the tail vein. When mannitol was used, a solution of 200 µl of sterile 25% mannitol in water was injected into the tail vein 8 minutes prior to virus injection. All injections were done in 8–12-week-old female BALB/c mice purchased from Jackson Laboratory (Bar Harbor, ME). Four weeks following vector injection, each mouse was killed and transcardially perfused with PBS or PBS containing 1 U/ml heparin (Abraxis, Schaumburg, IL). Organs were collected and processed for DNA extraction or immunolabeling. Blood was collected from mice according to Institutional Animal Care and Use Committee guidelines. To collect serum, the whole blood was incubated for 2 hours at room temperature followed by centrifugation at 1000*g* for 15 minutes. The supernatant (sera) was then stored at −80 °C. Once all sera were collected, they were tested for albumin, blood urea nitrogen, and ALT levels by the UNC Animal Clinical Laboratory Core Facility.

Immunolabeling and imaging of mouse samples: After 48 hours of fixation in freshly made PBS with 4% paraformaldehyde, the entire brain and portions of the cervical and lumbar spinal cords were sectioned at 40 µm using a Leica vibrating microtome at room temperature. To enhance the signal observed with GFP, every 5th section was processed for IHC. Samples were incubated for 1 hour at room temperature in blocking solution (10% goat serum, 0.1% Triton X-100, 1× PBS), then incubated for 48–72 hours at 4 °C in primary antibody solution [3% goat serum, 0.1% Triton X-100, 1× PBS, rabbit anti-GFP (# AB5541, 1:500; Millipore, Billerica, MA)]. After washing three times in 1× PBS, secondary amplification was performed using a VectaStain ABC Elite Kit (#PK-6101; Vector Labs, Burlingame, CA) with 3,3′-diaminobenzidine tetrachloride (#04008; Polysciences, Warrington, PA) substrate and nickel-cobalt intensification of the reaction product.

For co-labeling studies, blocking and primary antibody incubations were done as described above. After washing, the sections were incubated for 1 hour at room temperature in secondary antibody solution (3% goat serum, 0.1% Triton X-100, 1× PBS, secondary antibodies), then washed three more times in 1× PBS. Primary antibodies were as follows, with combinations described in **Figure 4**: rabbit anti-GFP (1:500, #AB5541; Millipore), mouse anti-NeuN (1:500, Millipore #MAB377), goat anti-ChAT (1:100, #AB144P; Millipore), and rabbit anti-Calbindin (1:500, #AB1778; Millipore). Secondary antibodies were as appropriate, each at 1:1000 dilution: goat anti-rabbit Alexa 488 (#A11008; Invitrogen, Carlsbad, CA), goat anti-mouse Alexa 594 (#A11032; Invitrogen), goat anti-rabbit Alexa 594 (#A11037; Invitrogen), donkey anti-goat Alexa 594 (#A11058; Invitrogen), and donkey anti-rabbit Alexa 594 (#A21206; Invitrogen).

Microscopy: Confocal imaging was performed at the Michael Hooker Microscopy Center at UNC-Chapel Hill using a Zeiss Axiovert LSM510 laser confocal microscope. Images were processed using Zeiss LSM Image Browser software. Dual-label immunofluorescence images were reconstructed from four consecutive steps in a Z-series taken at 1.3 µm intervals through the section of interest using a ×20 objective.

3,3′-diaminobenzidine tetrachloride-processed brain sections were digitized using a Scan-Scope slide scanner (Aperio Technologies, Vista, CA). Virtual slides were viewed using ImageScope software package (v. 10.0; Aperio Technologies), which allowed sections to be viewed at equivalent magnifications.

NHP studies

Animals and surgeries: Four juvenile (3–4-year-old) male rhesus macaques (*Macaca mulatta*) were used in this study and were cared for by the Division of Animal Resources at the Oregon National Primate Research Center in accordance with National Institutes of Health guidelines and approved by the Institutional Animal Care and Use Committee at OHSU. scAAV9-CBh-GFP at a dose of $0.9–1 \times 10^{13}$ vg/kg birth weight was injected in four NHPs on day 0 of the protocol, via two different systemic routes of administration (intravenous and intracarotid, $n = 2$). Animals were deeply anesthetized with ketamine HCl (10 mg/kg birth weight intramuscular injection) and anesthesia was maintained with isoflurane gas vaporized in 100% oxygen. For the intravenous injection ($n = 2$), a percutaneous 22-gauge

intravenous catheter was placed in the animal's right leg saphenous vein and flushed with saline to verify correct placement. The virus preparation, already diluted with a solution of PBS containing 5% sorbitol to a final volume of 10 ml/kg birth weight, was infused over a 15–20-minute period at a rate of 2.5 ml/minute. After the infusion was completed, the catheter was flushed with saline, removed, and digital pressure was applied on the puncture until complete hemostasis. After hemostasis is confirmed, each NHP was returned to his home cage for observation and recovery. Intracarotid infusion of scAAV9 was performed on two NHPs according to the following procedure. After administration of general anesthesia, pain transmission was blocked with a local anesthetic line block consisting of bupivacaine (0.25%) mixed with lidocaine (1%) and epinephrine (1:100,000) administered intradermally along the incision site. Once anesthesia was attained, a curvilinear 4 cm skin incision from the ventral midline of the neck extending to the medial aspect of the left mandibular ramus (condyle) was created. Blunt dissection through the subcutaneous tissue was followed by lateral retraction of the sternomastoid muscle, revealing the carotid trunk. The cranial nerve X (vagus) was dissected free from the common carotid artery, retracted with a vein loop. The right carotid trunk was dissected under the mandible to reveal the bifurcation of the internal, external, and lingual branches. A Rumel was placed around the external and lingual arteries, a 24-gauge catheter was introduced into the common carotid and a controlled infusion scAAV9-CBh-GFP diluted in PBS containing 5% sorbitol, at 10 ml/kg birth weight, was performed at a rate of 1.5 ml/minute. Once the infusion was complete the catheter was flushed with saline, the Rumels released and the catheter removed using digital pressure to provide hemostasis. After verification of hemostasis, the deep tissues, subcutaneous tissue and skin was apposed with running 4-0 Monocryl. Recovery occurred on the operating room table until extubation. Postoperative distress or pain was managed by hydromorphone (0.2 mg/kg intramuscular injections) administered every 4 hours for 24 hours, and buprenorphine (0.03 mg/kg intramuscular injections, at 2000 hours) to provide overnight analgesia. Animals were housed in Biosafety Level 2 facilities and in pairs when possible.

Necropsies and tissue dissection: Four weeks after virus administration, the four NHPs were euthanized following the recommendation from the Panel on Euthanasia of the American Veterinary Association. Each NHP was sedated with ketamine (10 mg/kg, intramuscular injection), given an overdose of barbiturate (25 mg/kg, intravenous injection) and killed by exsanguination. The brain was perfused through the ascending carotid artery with 1.5 l of heparinized saline solution (1 U/ml of heparin sodium, APP Pharmaceuticals, Schaumburg, IL, in 9.1 g NaCl/l) followed by 2.5 l of 4% paraformaldehyde (Electron Microscopy Sciences, Hatfield, PA) in PBS. Brains were removed from the skull and 4 mm coronal slabs, spanning the entire antero-posterior length of the brain were prepared using a monkey brain matrix (ASI Instruments, Warren, MI). Samples (1–2 cm^3) from different peripheral organs were also collected and either stored at 85 °C for molecular analysis or fixed by immersion in 4% paraformaldehyde for IHC and co-IF analysis.

Immunolabeling and imaging of NHP samples: After 48 hours of fixation in freshly made PBS with 4% paraformaldehyde, brain slabs were transferred in 30% sucrose-PBS solution. Anterior, medial and posterior 4 mm coronal slabs were sectioned at 40 µm using a Microm (Thermo Fisher Scientific, Kalamazoo, MI) sliding microtome. Portions of the thoracic spinal cords and various peripheral organs (liver, heart/ventricle, adrenals, kidney, spleen, testes) were also sectioned at 40 µm. GFP expression in these tissue samples was detected by IHC. Samples were washed in potassium phosphate-buffered saline (KPBS) buffer (0.02 mol/l, pH 7.4) and endogenous peroxidases were blocked by incubation for 30 minutes in KPBS-1% hydrogen peroxide, except for liver, spleen and kidney samples that were incubated in methanol-1% hydrogen peroxide. After three KPBS washes, sections were incubated for 30 minutes at room temperature in blocking solution (2% normal donkey serum, 0.5% Triton X-100, 0.02 mol/l KPBS), then incubated for 72 hours (brain sections) or 24 hours (all other samples) at 4 °C in primary antibody solution [2% normal donkey serum, 0.5% Triton X-100, 0.02 mol/l KPBS, goat anti-GFP (#ab6673, 1:1,500; Abcam, Cambridge, MA)]. After washing three times in 0.02 mol/l KPBS, secondary amplification was performed using a VectaStain ABC Elite Kit (#PK-6101; Vector Labs) with detection by diaminobenzidine tetrachloride (#D5905; Sigma, St Louis, MO) by itself or in conjunction with nickel sulfate hexahydrate (#N4882; Sigma). Stained sections were mounted on gelatin-coated slides and counterstained by incubation in a solution of 0.1% Cresyl Violet and 2.5% glacial acetic acid. Sections were then dehydrated and mounted in DPX mounting media.

For co-labeling studies, blocking and primary antibody incubations were done as described above. After washing, the sections were incubated for 1 hour at room temperature in secondary antibody solution (0.5% Triton X-100, 0.02M KPBS, secondary antibodies), then washed three more times in 1× PBS. Primary antibodies were as follows, with combinations described in **Figure 8**: goat anti-GFP (1:1,500, # ab6673; Abcam), mouse anti-glial fibrillary acidic protein (1:10,000, G3893; Sigma) and mouse anti-NeuN (1:500, #MAB377; Millipore). Secondary antibodies were used at 1:500 dilution and were: donkey anti-goat Alexa 488 (#A11055; Invitrogen) and goat anti-mouse Alexa 568 (#A11037; Invitrogen).

Simple IHC pictures were taken on a Zeiss Axioplan (Carl Zeiss Microimaging, Jena, Germany) coupled to a Retiga2000R camera managed by QCapture software (Qimaging, Surrey, BC, Canada). Imaging of double IHF was performed using a Zeiss Axio Imager 2 microscope linked to an Olympus DP71 camera managed by DP Controller software (v3.2.1.276, Olympus, Center Valley, PA).

NHP neutralizing antibody titer: HeLa RC32 cells (catalog # CRL-2972; ATCC, Manassas, VA) were seeded at 3×10^4 cells/well in a 48-well plate in Dulbecco's modified Eagle's medium with 10% fetal bovine serum and used the following day for the NAb experiment, at ~50% confluence. Serum samples from the NHP taken at preinjection (0 weeks), 1, 2, and 4 weeks were each serially diluted 1:2 in PBS. Ten microliters of each serum dilution was mixed with 10 µl of scAAV9/CBh-GFP (1.5×10^9 vg in PBS), then incubated for 2 hours at 4 °C. The AAV9/serum solution was mixed with 100 µl of adenovirus (5×10^5 infectious units) in Dulbecco's modified Eagle's medium and immediately added to the HeLa RC32 cells. After incubation at 37 °C for 48 hours, cells were visualized for GFP expression. The NAb titer reported is the serum dilution showing a 50% decrease in the number of GFP positive cells.

SUPPLEMENTARY MATERIAL

Figure S1. Comparison of AAV1, 5, 6, 8, and 9 for intravenous delivery to the mouse CNS with mannitol.
Figure S2. IHC of non-transduced CNS tissue.
Figure S3. Enlarged image of **Figure 1c**, right panel.
Figure S4. Enlarged image of **Figure 1d**, right panel.
Figure S5. Enlarged image of **Figure 1e**, right panel.
Figure S6. Darker exposure (DAB reaction) of a different hippocampus slice portrayed in **Figure 1b**, right panel.
Figure S7. Darker exposure (DAB reaction) of a different striatum slice portrayed in **Figure 1c**, right panel.
Figure S8. Darker exposure (DAB reaction) of a different cerebellum slice portrayed in **Figure 1d**, right panel.
Figure S9. ssAAV9 can transduce the mouse CNS, but at a much lower efficiency.
Figure S10. Astrocyte transduction in NHPs.
Figure S11. Neuron transduction in NHPs.
Figure S12. Staining of neuron-like cells in i.c. versus i.v. injected NHPs.
Table S1. Fold differences and *P* values corresponding to **Figure 1a**.
Table S2. Neuron versus astrocyte counts in mice and nonhuman primates.
Table S3. Vector persistence in the serum of injected nonhuman primates.

Table S4. AAV-packaged constructs used.

ACKNOWLEDGMENTS

This work was supported by generous grants from the ALS Association, the International Rett Syndrome Foundation, Hannah's Hope Fund, the Senator Paul D. Wellstone Muscular Dystrophy Cooperative Research Center Grant U54-AR056953, and the Oregon National Primate Research Center Core grant RR000163. We thank Kelly Shaw, Bonita Blake, and Joel Schwartz for technical assistance. We thank Chengwen Li for helpful discussions on AAV-relevant immunology. We would like to acknowledge Jim Wilson's group at the University of Pennsylvania for the discovery of AAV9, and thank Dr Xiao at University of North Carolina (UNC) and the UNC Vector Core for providing the AAV9 helper plasmid.

REFERENCES

1. Rubin, LL and Staddon, JM (1999). The cell biology of the blood-brain barrier. *Annu Rev Neurosci* **22**: 11–28.
2. Rapoport, SI (2000). Osmotic opening of the blood-brain barrier: principles, mechanism, and therapeutic applications. *Cell Mol Neurobiol* **20**: 217–230.
3. Fu, H, Kang, L, Jennings, JS, Moy, SS, Perez, A, Dirosario, J *et al.* (2007). Significantly increased lifespan and improved behavioral performances by rAAV gene delivery in adult mucopolysaccharidosis IIIB mice. *Gene Ther* **14**: 1065–1077.
4. Fu, H, Muenzer, J, Samulski, RJ, Breese, G, Sifford, J, Zeng, X *et al.* (2003). Self-complementary adeno-associated virus serotype 2 vector: global distribution and broad dispersion of AAV-mediated transgene expression in mouse brain. *Mol Ther* **8**: 911–917.
5. McCarty, DM, DiRosario, J, Gulaid, K, Muenzer, J and Fu, H (2009). Mannitol-facilitated CNS entry of rAAV2 vector significantly delayed the neurological disease progression in MPS IIIB mice. *Gene Ther* **16**: 1340–1352.
6. Duque, S, Joussemet, B, Riviere, C, Marais, T, Dubreil, L, Douar, AM *et al.* (2009). Intravenous administration of self-complementary AAV9 enables transgene delivery to adult motor neurons. *Mol Ther* **17**: 1187–1196.
7. Foust, KD, Nurre, E, Montgomery, CL, Hernandez, A, Chan, CM and Kaspar, BK (2009). Intravascular AAV9 preferentially targets neonatal neurons and adult astrocytes. *Nat Biotechnol* **27**: 59–65.
8. Towne, C, Raoul, C, Schneider, BL and Aebischer, P (2008). Systemic AAV6 delivery mediating RNA interference against SOD1: neuromuscular transduction does not alter disease progression in fALS mice. *Mol Ther* **16**: 1018–1025.
9. Foust, KD, Wang, X, McGovern, VL, Braun, L, Bevan, AK, Haidet, AM *et al.* (2010). Rescue of the spinal muscular atrophy phenotype in a mouse model by early postnatal delivery of SMN. *Nat Biotechnol* **28**: 271–274.
10. Zincarelli, C, Soltys, S, Rengo, G and Rabinowitz, JE (2008). Analysis of AAV serotypes 1-9 mediated gene expression and tropism in mice after systemic injection. *Mol Ther* **16**: 1073–1080.
11. McCarty, DM, Fu, H, Monahan, PE, Toulson, CE, Naik, P and Samulski, RJ (2003). Adeno-associated virus terminal repeat (TR) mutant generates self-complementary vectors to overcome the rate-limiting step to transduction in vivo. *Gene Ther* **10**: 2112–2118.
12. McCarty, DM, Monahan, PE and Samulski, RJ (2001). Self-complementary recombinant adeno-associated virus (scAAV) vectors promote efficient transduction independently of DNA synthesis. *Gene Ther* **8**: 1248–1254.
13. Gordon, N (2004). Giant axonal neuropathy. *Dev Med Child Neurol* **46**: 717–719.
14. Yang, Y, Allen, E, Ding, J and Wang, W (2007). Giant axonal neuropathy. *Cell Mol Life Sci* **64**: 601–609.
15. Jiang, H, Couto, LB, Patarroyo-White, S, Liu, T, Nagy, D, Vargas, JA *et al.* (2006). Effects of transient immunosuppression on adenoassociated, virus-mediated, liver-directed gene transfer in rhesus macaques and implications for human gene therapy. *Blood* **108**: 3321–3328.
16. Wang, L, Calcedo, R, Wang, H, Bell, P, Grant, R, Vandenberghe, LH *et al.* (2010). The pleiotropic effects of natural AAV infections on liver-directed gene transfer in macaques. *Mol Ther* **18**: 126–134.
17. Manno, CS, Pierce, GF, Arruda, VR, Glader, B, Ragni, M, Rasko, JJ *et al.* (2006). Successful transduction of liver in hemophilia by AAV-Factor IX and limitations imposed by the host immune response. *Nat Med* **12**: 342–347.
18. Hasbrouck, NC and High, KA (2008). AAV-mediated gene transfer for the treatment of hemophilia B: problems and prospects. *Gene Ther* **15**: 870–875.
19. Mingozzi, F and High, KA (2007). Immune responses to AAV in clinical trials. *Curr Gene Ther* **7**: 316–324.
20. Jiang, H, Pierce, GF, Ozelo, MC, de Paula, EV, Vargas, JA, Smith, P *et al.* (2006). Evidence of multiyear factor IX expression by AAV-mediated gene transfer to skeletal muscle in an individual with severe hemophilia B. *Mol Ther* **14**: 452–455.
21. Manno, CS, Chew, AJ, Hutchison, S, Larson, PJ, Herzog, RW, Arruda, VR *et al.* (2003). AAV-mediated factor IX gene transfer to skeletal muscle in patients with severe hemophilia B. *Blood* **101**: 2963–2972.
22. Gray, SJ, Blake, BL, Criswell, HE, Nicolson, SC, Samulski, RJ, McCown, TJ *et al.* (2010). Directed evolution of a novel adeno-associated virus (AAV) vector that crosses the seizure-compromised blood-brain barrier (BBB). *Mol Ther* **18**: 570–578.
23. Breous, E, Somanathan, S and Wilson, JM (2010). BALB/c mice show impaired hepatic tolerogenic response following AAV gene transfer to the liver. *Mol Ther* **18**: 766–774.
24. Lu, Y and Song, S (2009). Distinct immune responses to transgene products from rAAV1 and rAAV8 vectors. *Proc Natl Acad Sci USA* **106**: 17158–17162.
25. Wu, Z, Asokan, A, Grieger, JC, Govindasamy, L, Agbandje-McKenna, M and Samulski, RJ (2006). Single amino acid changes can influence titer, heparin binding, and tissue tropism in different adeno-associated virus serotypes. *J Virol* **80**: 11393–11397.
26. Asokan, A, Conway, JC, Phillips, JL, Li, C, Hegge, J, Sinnott, R *et al.* (2010). Reengineering a receptor footprint of adeno-associated virus enables selective and systemic gene transfer to muscle. *Nat Biotechnol* **28**: 79–82.
27. Pulicherla, N, Shen, S, Yadav, S, Debbink, K, Govindasamy, L, Agbandje-McKenna, M *et al.* (2011). Engineering Liver-detargeted AAV9 Vectors for Cardiac and Musculoskeletal Gene Transfer. *Mol Ther* (epub ahead of print).
28. Cearley, CN, Vandenberghe, LH, Parente, MK, Carnish, ER, Wilson, JM and Wolfe, JH (2008). Expanded repertoire of AAV vector serotypes mediate unique patterns of transduction in mouse brain. *Mol Ther* **16**: 1710–1718.
29. Baker, AH, Mcvey, JH, Waddington, SN, Di Paolo, NC and Shayakhmetov, DM (2007). The influence of blood on *in vivo* adenovirus bio-distribution and transduction. *Mol Ther* **15**: 1410–1416.
30. Shayakhmetov, DM, Gaggar, A, Ni, S, Li, ZY and Lieber, A (2005). Adenovirus binding to blood factors results in liver cell infection and hepatotoxicity. *J Virol* **79**: 7478–7491.
31. Boutin, S, Monteilhet, V, Veron, P, Leborgne, C, Benveniste, O, Montus, MF *et al.* (2010). Prevalence of serum IgG and neutralizing factors against adeno-associated virus (AAV) types 1, 2, 5, 6, 8, and 9 in the healthy population: implications for gene therapy using AAV vectors. *Hum Gene Ther* **21**: 704–712.
32. Scallan, CD, Jiang, H, Liu, T, Patarroyo-White, S, Sommer, JM, Zhou, S *et al.* (2006). Human immunoglobulin inhibits liver transduction by AAV vectors at low AAV2 neutralizing titers in SCID mice. *Blood* **107**: 1810–1817.
33. Li, W, Asokan, A, Wu, Z, Van Dyke, T, DiPrimio, N, Johnson, JS *et al.* (2008). Engineering and selection of shuffled AAV genomes: a new strategy for producing targeted biological nanoparticles. *Mol Ther* **16**: 1252–1260.
34. Maheshri, N, Koerber, JT, Kaspar, BK and Schaffer, DV (2006). Directed evolution of adeno-associated virus yields enhanced gene delivery vectors. *Nat Biotechnol* **24**: 198–204.
35. Sands, MS and Haskins, ME (2008). CNS-directed gene therapy for lysosomal storage diseases. *Acta Paediatr Suppl* **97**: 22–27.
36. Gray, SJ, Woodard, KT and Samulski, RJ (2010). Viral vectors and delivery strategies for CNS gene therapy. *Ther Deliv* **1**: 517–534.
37. Grieger, JC, Choi, VW and Samulski, RJ (2006). Production and characterization of adeno-associated viral vectors. *Nat Protoc* **1**: 1412–1428.